Thermodynamic Aspects of Fatty Acids Binding to Human Serum Albumin: A Microcalorimetric Investigation

Hatsumi AKI and Magobei YAMAMOTO*

Faculty of Pharmaceutical Sciences, Fukuoka University, 8–19–1 Nanakuma, Jonan-ku, Fukuoka 814–01, Japan. *Received October 21, 1991*

Thermodynamic parameters have been evaluated for the binding interaction between human serum albumin (HSA) and unbranched fatty acids (FFA) on the basis of a flow microcalorimetric measurement at pH 7.4 and 37 °C by computer-fitting to single- and two-class binding models. The heat of binding increased exothermically with increasing alkyl chain length. FFA with nine or less carbons bound to only one class of binding sites ($n=2$) with a binding constant (K) of $10^4\,M^{-1}$. FFA with ten or more carbons bound to the first class of binding sites with high affinity K in the order of 10^5 to $10^6\,M^{-1}$, and to the second class with a lower affinity and high capacity. The free energy change of the first class of binding sites (ΔG_1) became more negative as the chain length of FFA was increased. The enthalpy change per mol of FFA (ΔH) decreased at the rate of $-7.47\,kJ\cdot mol^{-1}\cdot CH_2^{-1}$ to a minimum at C9 and then increased due to the hydrophobicity of alkyl chains. Compensation analysis for the i th class of HSA molecule by plotting molar changes of enthalpy (ΔH_{mi}) against entropy (ΔS_{mi}) and free energy (ΔG_{mi}) indicates two distinct binding sites. The first class ($i=1$) of the long-chain FFA on HSA is an entropy-driven reaction associated with nearly constant values of ΔH_{m1} ($-43.0\pm4.8\,kJ\cdot mol^{-1}$), slightly negative values of ΔS_{m1} ($-47.4\leqq\Delta S_{m1}\leqq-8.1\,J\cdot mol^{-1}\cdot K^{-1}$) and $-\Delta G_{m1}$ values, increasing with increasing alkyl chain length. The second class ($i=2$) of the long-chain FFA may lie in the same region as the binding sites of the short- and medium-chain FFA with a linear relationship between ΔH_{mi}–ΔS_{mi}.

Keywords unbranched fatty acid; HSA; binding interaction; flow microcalorimetry; ultrafiltration; thermodynamic parameter (ΔG, ΔH, ΔS); binding parameter (K, n)

Introduction

Free fatty acids (FFA) interact with various binding sites of human serum albumin (HSA) *in vivo*.[1–4] Their binding isotherms,[4–13] location of the binding sites,[14–17] competitive displacement[18–24] and allosteric effects[25,26] have been extensively studied. The interactions of ionic ligands bearing alkyl side chains to the protein can be attributed to the hydrophobic character of the alkyl chain, and hydrogen bonding, van der Waals' and electrostatic forces, which are due to the charged group.[27,28] The unbranched carboxylic fatty acids provide a convenient homologous series of ligand molecules with a carboxy anion group at one end but with varying alkyl chain length/hydrophobicity.

In the binding phenomena, the free energy changes (ΔG) calculated from the binding constant are only slightly dependent on changes in the molecular details of the reaction, while the corresponding enthalpy values (ΔH) and entropy changes (ΔS) are much more sensitive and give a more complete characterization of interactions.[29–31] In only a few instances, the enthalpy and entropy changes of FFA binding have been determined in the normal way, by measuring the variation of the binding constant with temperature.[7,8,16] This data has been interpreted in terms of the changes in the absolute value of the thermodynamic parameters as conditions are changed, rather than in terms of the fundamental meaning of the parameters. No evidence has yet been presented of any systematic relation among thermodynamic parameters.

Several reports on drug binding[32–35] have so far suggested the usefulness of flow microcalorimetry, which we first applied to the thermodynamic behavior of ionic drug interactions in the blood system.[36–40] The potential advantage of microcalorimetric titration is that the method directly measures the "heat signal" occurence of the binding process and thereby avoids the need to partition between free and bound drug ligands. The heat signal gives a quantity proportional to the amount of binding reaction, so it is the only technique which allows simultaneous determination of all binding and thermodynamic parameters in a single experiment.[36] In the present work, we studied the binding of a consecutive FFA to HSA by a flow microcalorimetric method, and provided a thermodynamic description based on the complex-forming reaction.

Experimental

Materials HSA (HSA fraction V, "essentially fatty acid free," less than 0.005% fatty acids) obtained from Sigma (St. Louis, MO, U.S.A.) was used without further purification. HSA was dissolved in a 1/30 M phosphate buffer, pH 7.4, and its molecular weight was assumed to be 69000. All FFA were supplied from Nippon Chromato Kogyo Co., Ltd. (Tokyo, Japan). A relatively concentrated solution of each acid dissolved in 0.01 N NaOH was prepared and diluted with a 1/30 M phosphate buffer, pH 7.4, to provide the desired initial concentration (10^{-6} to 10^{-3} M). The initial pH of all solutions was adjusted to the range of 7.40 to 7.46. 1-^{14}C-Caproic acid with a specific activity of 14.9 mCi/mmol and 1-^{14}C-lauric acid with 36.3 mCi/mmol were purchased from New England Nuclear Co. (Boston, MA, U.S.A.) and Amersham International plc (Buckinghamshire, U.K.), respectively. The radiochemical and chemical purities were checked by Packard Radiochromatogram Scanner System 7201 (Downers Grove, IL, U.S.A.).

Microcalorimetry Calorimetric experiments were carried out at 37.0 ± 0.005 °C using an adiabatic differential flow microcalorimeter with a twin-cell structure. Details of this calorimeter and its operation mode were described previously.[36] The reaction solutions were introduced at a constant flow rate ($0.12\,ml\cdot min^{-1}$) into the calorimeter through Tygon tubing using a Gilson minipuls 2 peristaltic pump (Villers-Le-Bel, France). A base line was established by flowing phosphate buffer and HSA in the buffer solution, corresponding to the heat of dilution of HSA. The initial and final concentrations of HSA were determined by the adsorption at 278 nm using an extinction coefficient $E_{278}^{0.1\%}$ of 0.531. Consequently, the final HSA concentrations were equal to half of the initial concentrations. FFA solutions at different concentrations were then introduced sequentially into the buffer flow line in the reaction cell. The heat effect was proportional to the recorded steady-state value (maximum deviation). The calorimetric calibration was carried out by introducing a known quantity of electric power into the electric calibration heater.

Calculation of Thermodynamic Parameters The heat of FFA ligand binding to HSA protein was measured as a function of ligand concentration (L). The experimental heat effect (W) associated with mixing of the reactants is related to the heat of binding (Q_b), the heat of dilution of

the protein and ligand (Q_{dil}), and the heat associated with the physical mixing of solutions (Q_{mix}).

$$W=Q_b+Q_{dil}+Q_{mix} \quad (1)$$

The heat of dilution and mixing of the protein can be instrumentally eliminated. After subtraction of the heat of dilution and mixing of the ligand measured separately, the heat of binding is proportional to the quantity of ligand–protein complex formed with the protein concentration fixed at P, as follows[30]:

$$Q_b=\Delta H\cdot L_b\cdot F_r \quad (2)$$

where ΔH is the binding enthalpy per mole of ligand and L_b is a bound concentration of the ligand at a constant flow rate of F_r. The equilibrium aspect of such interactions was correlated through the mass action law, yielding the familiar equation:

$$r=L_b/P=\sum_{i=1}^{\hat{m}}(n_i\cdot K_i\cdot L_f)/(1+K_i\cdot L_f) \quad (3)$$

where m is the number of classes of independent binding sites such that each class (i) has n_i sites with the binding constant (K_i), and the free ligand concentration (L_f) is related to the equation,

$$L=L_b+L_f \quad (4)$$

For a single-class binding model (m=1), the general Eq. 3 becomes

$$Q_b=\Delta H\cdot F_r(A-\sqrt{A^2-4n_1\cdot P\cdot L})/2 \quad (5)$$

where

$$A=1/K_1+n_1\cdot P+L \quad (6)$$

For a two-class binding model (m=2), Eq. 3 reduces to

$$L_f^3+A\cdot L_f^2+B\cdot L_f+C=0 \quad (7)$$

where

$$A=P(n_1+n_2)+(1/K_1+1/K_2)-L$$
$$B=P(n_1/K_2+n_2/K_1)-L(1/K_1+1/K_2)+1/K_1\cdot 1/K_2$$
$$C=-L/K_1\cdot 1/K_2 \quad (8)$$

The binding and thermodynamic parameters, K_i, n_i and ΔH, can be computed from actual calorimetric data by an iterative non-linear least-squares regression program for minimizing the value of $\Sigma(Q_{b,exp}-Q_{b,calc})^2$. The initial estimates of ΔH are obtained from the slope of the initial linear part of a calorimetric titration curve with excess protein.[37] All procedures were carried out with a FACOM M-380R computer at Fukuoka University.

Ultrafiltration The binding studies of caproic acid (C6) and lauric acid (C12) with HSA were carried out using a technique of ultrafiltration with Amicon Centriflo membrane cones CF-25 (Lexington, MA, U.S.A.) as previously described.[41] The membrane cones were soaked in distilled water overnight before use. After removing the water on the membrane by centifugation, 2.0 ml of 2% HSA solution was added into the cone and a small volume of concentrated FFA solution containing a tracer amount of radiolabeled FFA was then added. Following incubation for 30 min at 37.0 °C, the solution was centrifuged at 1000 *g* for 20 min and 0.5 ml of ultrafiltrated solution was taken for radioactive counting by use of a Packard TRI-CARB 2660 liquid scintillation spectrometer (Downers Grove, IL, U.S.A.) to determine the free and bound concentrations of FFA. The extent of FFA binding to HSA was measured over a range of from 10^{-6} to 10^{-3} M of FFA. In order to calculate the binding parameters, computer fitting of experimental data to a two-class binding model Eq. 3 (m=2) was performed.

Results

Stoichiometry of Fatty Acid Binding to HSA Figures 1 and 2 show the calorimetric titrations of HSA with caproic (C6) and lauric acid (C12) at several concentrations of HSA, respectively. The curves were obtained by a computer curve-fitting procedure assuming the single-class binding model. The estimated values of the binding and thermodynamic parameters are listed in Table I, together with MSE (a mean of squared prediction errors). The parameter ΔH_{max} in Table I represents the molar enthalpy change of HSA for complete binding of all sites, and the value was estimated from a plateau value ($Q_{b,max}$) of a calorimetric titration curve by using the equation:

$$Q_{b,max}=\Delta H_{max}\cdot F_r\cdot P \quad (9)$$

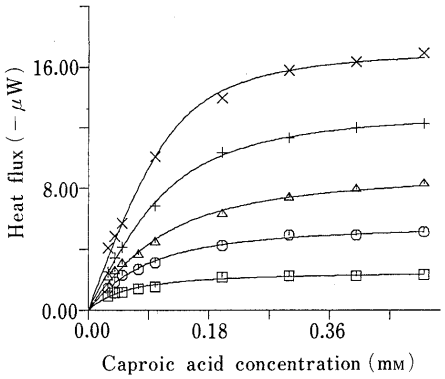

Fig. 1. Heat Produced during Titrations of HSA with Caproic Acid at 37 °C and pH 7.4 in 1/30 M Phosphate Buffer

The initial concentrations of HSA used were 0.15% (□—□), 0.25% (○—○), 0.50% (△—△), 0.75% (+—+) and 1.00% (×—×) (w/v). Each point is an average of three measurements and solid lines represent the fitting curves drawn by a computer assuming a single-class binding model.

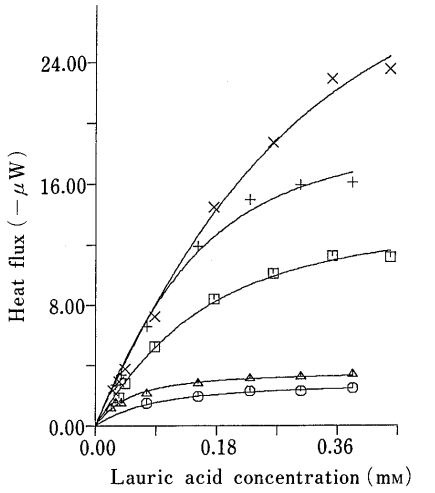

Fig. 2. Heat Produced during Titrations of HSA with Lauric Acid at 37 °C and pH 7.4 in 1/30 M Phosphate Buffer

The initial concentrations of HSA used were 0.05% (○—○), 0.08% (△—△), 0.20% (□—□), 0.25% (+—+) and 0.40% (×—×) (w/v). Each point is an average of three measurements and solid lines represent the fitting curves drawn by a computer assuming a single-class binding model.

Table I. Binding Parameters Estimated from Calorimetric Titration Curves of Caproic and Lauric Acid Binding to HSA Assuming Single-Class Binding Model

Fatty acid	HSA (%)	K (10^4/M)	n	$-\Delta H$ (kJ/mol)	$-\Delta H_{max}$ (kJ/mol)	MSE
Caproic acid	0.15	2.151	1.8	37.7	69.8	0.0178
	0.25	1.583	2.0	37.7	78.4	0.0211
	0.50	1.950	2.1	35.0	75.2	0.0497
	0.75	2.508	2.2	35.0	78.4	0.0314
	1.0	2.877	1.7	39.0	69.5	0.0634
Lauric acid	0.05	1.364	6.9	38.9	266.8	0.0180
	0.08	3.106	6.2	43.4	270.5	0.0295
	0.20	1.332	7.2	44.9	330.1	0.0957
	0.25	1.979	7.3	41.2	325.9	0.107
	0.40	0.810	8.4	41.2	352.8	0.113

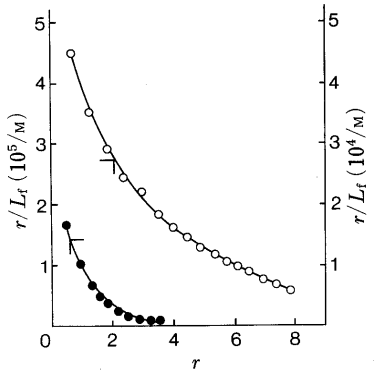

Fig. 3. Scatchard Plots of Interaction of HSA with Caproic and Lauric Acid at 37 °C Determined by Ultrafiltration

Points represent the mean value of r and r/L_f determined from five estimates at the same total concentration of C6 (●) and C12 (○) acid. Caproic acid; $K_1=1.445\times10^4\,M^{-1}$, $K_2=0.776\times10^2\,M^{-1}$, $n_1=1.6$ and $n_2=9.0$. Lauric acid; $K_1=8.219\times10^4\,M^{-1}$, $K_2=0.443\times10^4\,M^{-1}$, $n_1=1.0$ and $n_2=9.0$.

The figures obtained for ΔH_{max} were compared with total amounts of the binding enthalpy change of all binding sites, $n\cdot\Delta H$ (Table I). The agreement between the two values is an argument in favor of the validity of the mathematical model, indicating that n represents the molar ratio of FFA to HSA for the complexation and that ΔH_{max} is the extent of the binding area or binding capacity on the HSA molecule.

Calorimetric data of C6 at every concentration of HSA fitted well to the single-class binding model with small values of MSE as shown in Table I. The heat of binding increased in proportion to the concentration of HSA and appeared to be saturated at a higher concentration of C6. The binding and thermodynamic parameters computed were essentially constant at all concentrations of HSA investigated in this study; $K=2.214\pm0.448\times10^4\,M^{-1}$, $n=1.96\pm0.19$, $\Delta H=-36.9\pm1.6\,kJ\cdot mol^{-1}$ and $\Delta H_{max}=-74.3\pm3.9\,kJ\cdot mol^{-1}$. On the other hand, the heat of binding of C12 to HSA was highly exothermic and the data fitted poorly to the model with a large MSE at a higher concentration of HSA ($\geqq0.2\%$). Also, the values of n and ΔH_{max} increased by increasing the concentration of HSA (Table I).

Another reliable determination of the binding parameters can be obtained from the binding data using the ultrafiltration technique at a very low FFA-to-HSA ratio. These compared to the results from calorimetric data. Figure 3 illustrates Scatchard plots for C6 and C12 binding to 2% HSA. Scatchard analysis of C6 binding indicates two classes of binding sites: $K_1=1.445\times10^4\,M^{-1}$ and $n_1=1.6$ and with $K_2=0.776\times10^2\,M^{-1}$, $n_2=9.0$. The value of K_1 was 200-fold higher than that of K_2, and the binding parameters obtained for the first class agreed with the results from the calorimetric data. Thus, C6 was bound to the primary sites and only to a small extent, or not at all, to the secondary sites. For the binding of C12, the presence of two classes of independent binding sites were clearly shown in Scatchard analysis; $K_1=41.10\times10^4\,M^{-1}$ and $n_1=1.0$ for the first class and $K_2=2.215\times10^4\,M^{-1}$ and $n_2=9.0$ for the second class. Considering that the calorimetric data did not fit a single-class binding model at higher concentrations of HSA, the binding sites of C12 on the HSA molecule are not built up from only a single class, but from two or more classes, and the heat effect appeared to be the sum of both Q_b for at least two classes of binding sites.

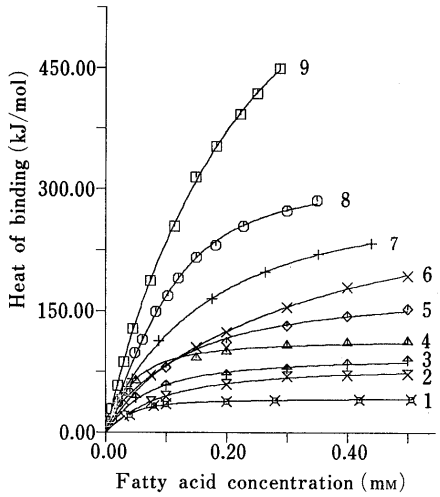

Fig. 4. Heat of Binding of Fatty Acids to HSA at 37 °C and pH 7.4 in 1/30 M Phosphate Buffer

The initial concentrations of HSA used were about 0.2% (w/v) and the final concentrations in the calorimetric solutions were determined to be 1.41 to 1.50×10^{-5} M. Solid lines represent computer-fitting curves assuming a two-class binding model. 1, butyric acid; 2, caproic acid; 3, caprylic acid; 4, pelargonic acid; 5, capric acid; 6, undecylic acid; 7, lauric acid; 8, myristic acid; 9, palmitic acid.

TABLE II. Binding and Thermodynamic Parameters of Fatty Acids Binding to HSA in 1/30 M Phosphate Buffer, pH 7.4 and 37 °C

Fatty acids	$-\Delta H$ (kJ/mol)	K_1 (10^4/M)	n_1	K_2 (10^3/M)	n_2
Butyric acid	23.74±2.27	1.110±0.161	2.3	—	—
Caproic acid	36.22±2.55	1.652±0.096	2.3	—	—
Caprylic acid	53.45±1.05	2.579±0.476	1.9	—	—
Pelargonic acid	60.36±1.18	3.106±0.927	1.5	—	—
Capric acid	51.71±2.02	14.40 ±1.368	0.9	4.829±0.187	3.2
Undecylic acid	46.35±0.13	29.40 ±0.264	0.8	5.922±0.122	5.4
Lauric acid	42.73±2.66	49.83 ±0.434	0.9	9.008±0.070	5.6
Myristic acid	39.61±2.59	113.2 ±0.564	1.1	17.09 ±1.003	5.5
Palmitic acid	38.90±2.60	216.8 ±2.680	1.2	22.66 ±1.055	6.7

The initial concentrations of HSA were 0.20%. Each value is the mean of best fit values calculated from three calorimetric titration curves using single- and two-class binding model.

Heat of Binding of Fatty Acids to HSA The results of calorimetric titrations of HSA with consecutive saturated FFA, butyric acid (C4) through palmitic acid (C16), are shown in Fig. 4, where the solid lines represented computer-generated best fit curves using a two-class binding model. The initial concentration of HSA used was about 0.2%. The calorimetric data was better presented by a plot of the heat of binding per mole of HSA ($kJ\cdot mol^{-1}$) *vs.* the total concentrations of FFA. The calorimetric data was examined by computer-fitting to both single- and two-class binding models, and the most probable values of binding parameters were listed in Table II.

The heat of binding increased exothermically with increasing the alkyl chain length of FFA as shown in Fig. 4. In every case of FFA with nine or less carbons (C4 to C9), the calorimetric data fitted well to both models with a small MSE. However, the values of n_1 computed from the two-class binding model were much smaller than 0.5, indicating that HSA had either no or a very small available binding site for the first class of binding site in the two-class

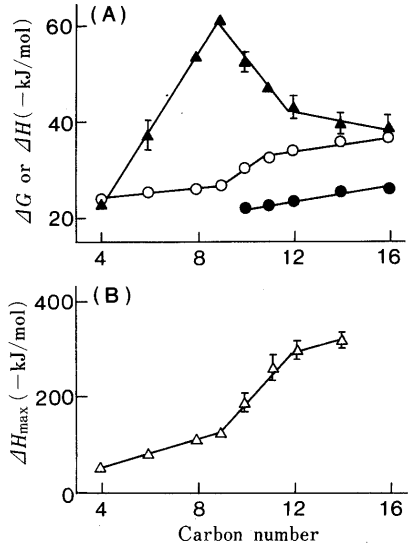

Fig. 5. Influence of Fatty Acid Chain Length on Thermodynamic Parameters of Fatty Acids Binding to HSA

The value of free energy change (ΔG) was calculated from the binding constant (K) listed in Table II using Eq. 10. Enthalpy change per mol of fatty acid (ΔH) and enthalpy change per mol of HSA (ΔH_{max}) were determined directly from individual calorimetric titration. ○, ΔG_1; ●, ΔG_2; ▲, ΔH; △, ΔH_{max}.

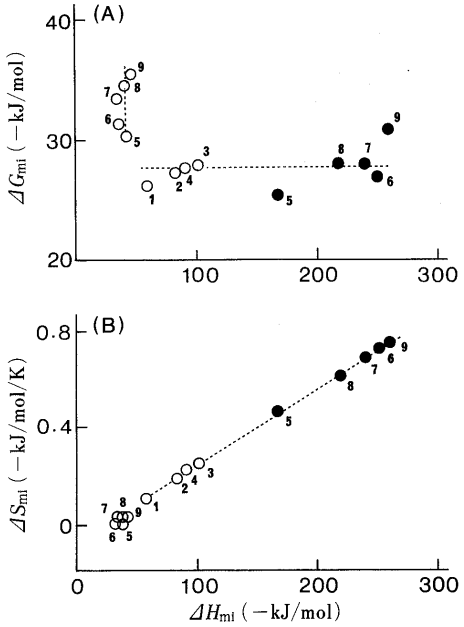

Fig. 6. Compensation Analysis Using (A) Molar Changes of Enthalpy (ΔH_{mi}) and Free Energy (ΔG_{mi}) Coordinates and (B) Enthalpy/Entropy (ΔS_{mi}) Coordinates for Each Class of HSA Binding Sites of Fatty Acids

The numbers refer to Fig. 4 legend. ○, the first class; ●, the second class of binding sites on HSA molecule.

binding model. The binding parameter, K_2 and n_2 of the second class, agree with those from the model assuming a single class of binding sites. By contrast, the calorimetric data for FFA with ten or more carbons (C10 to C16) did not fit the single-class binding model. Using a two-class binding model with independent binding sites, a better fit was observed between data and the curves generated with K_1, K_2, n_1 and n_2 in Table II.

Effect of Alkyl Chain Length on the Thermodynamic Parameters for Fatty Acid Binding to HSA The heat of binding and the binding affinities of FFA for HSA increased significantly with increasing alkyl chain length in the binding process. The relationships between thermodynamic parameters and alkyl chain length of FFA are shown in Fig. 5. Free energy change of the i th class of binding sites (ΔG_i) was calculated from the following equation:

$$\Delta G_i = -\boldsymbol{R}\cdot T\cdot \ln K_i \quad (10)$$

where $\boldsymbol{R}$ is the gas constant and T is the temperature in Kelvin. The value of $-\Delta G_1$ increased gradually from C4 to C9 with an increment of 538 J·mol^{-1}, and from C11 to C16 with 1.02 kJ·mol^{-1} per methylene group. However, a large increase in the value of $-\Delta G_1$ between C9 and C11 was observed with 2.90 kJ·mol^{-1}·CH_2^{-1} (Fig. 5A). The $-\Delta G_2$ value increased with increasing alkyl chain length at an increment amounting to 610 J·mol^{-1}·CH_2^{-1}. The parameters of ΔH and ΔH_{max}, estimated directly from the calorimetric titration curves, were independent of the binding model, and these variations were much larger than those of ΔG. The value of $-\Delta H$ steeply increased at the rate of 7.47 kJ·mol^{-1}·CH_2^{-1} to a maximum at C9 and then gradually reduced and leveled off as the chain length became longer (Fig. 5A). In contrast, the chain length dependence of ΔH_{max} showed quite a similar tendency to that of ΔG_1. The value of $-\Delta H_{max}$ increased steadily from C4 to C9 and C11 to C16 but there is a disproportionately large increase in $-\Delta H_{max}$ between C9 and C11 (Fig. 5B).

Thermodynamics for the Binding of Fatty Acids to HSA To characterize the FFA binding sites on HSA, a compensation analysis was examined by plotting ΔH_{mi} against ΔS_{mi} and ΔG_{mi}, representing the molar enthalpy, entropy and free energy changes of HSA for the i th class of binding sites, respectively. The values were calculated by the following equations.[30,37,40]

$$\Delta H_{mi} = n_i\cdot \Delta H$$
$$\Delta G_{mi} = -\boldsymbol{R}\cdot T\cdot \ln (n_i\cdot K_i)$$
$$\Delta S_{mi} = (\Delta H_{mi} - \Delta G_{mi})/T \quad (11)$$

As shown in Fig. 6, ΔH_{mi}–ΔS_{mi} plots are represented by two independent linear relations for the first class and for the second class of binding sites of FFA (≧C10). The first class of binding sites with a high affinity constant K_1 was characterized by a relatively constant enthalpy change ($\Delta H_{m1} = -43.0 \pm 4.8$ kJ·mol^{-1}) and a slight negative entropy change ($-47.4 \leqq \Delta S_{m1} \leqq -8.1$ J·mol^{-1}·K^{-1}). The second class having a lower affinity was characterized by dual large negative values of ΔH_{m2} (-261.4 to -167.0 kJ·mol^{-1}) and ΔS_{m2} (-744 to -458 J·mol^{-1}·K^{-1}). For FFA (≦C9), with only a single class of binding sites on HSA, the ΔH_{mi}–ΔS_{mi} plots lie on the same straight line passing those of the second class of FFA≧C10 ($\Delta H_{mi} = 0.313\Delta S_{mi} + 26.3$, $r = 0.9998$). The values of ΔH_{mi} and ΔS_{mi} ranged between -103.2 and -54.4 kJ·mol^{-1} and between -242.9 and -91.1 J·mol^{-1}·K^{-1}, respectively.

The plot of ΔG_{mi} against ΔH_{mi} (Fig. 6A) was divided into two groups, pointing to a clear difference in the binding sites. The first class of binding sites for FFA (≧C10) was associated with a constant ΔH_{m1}, but the $-\Delta G_{m1}$ value increased with increasing alkyl chain length. Meanwhile, in the second class of FFA (≧C10) and the first class of FFA (≦C9), the values of ΔG_{mi} were almost constant,

$-27.6 \pm 1.6\,kJ \cdot mol^{-1}$, despite the fact that ΔH_{mi} varied in the large range.

Discussion

Results from the calorimetric data show the disparate stoichiometry of FFA binding to HSA; short- and medium-chain FFA ($\leqq$C9) are bound to a single class of binding sites to form a FFA–HSA complex at a ratio of 2:1 with a K of $10^4\,M^{-1}$, while long-chain FFA ($\geqq$C10) have at least two classes of independent binding sites which contain only one strong binding site with K_1 in the order of 10^5 to $10^6\,M^{-1}$, and some weak sites from K_2 of 10^3 to $10^4\,M^{-1}$ (Table II).

The strength of FFA binding to HSA increases with the alkyl chain length of FFA, but the increase is non-proportional in $-\Delta G_1$ for FFA containing 4 to 16 carbon atoms; the increments per methylene group of $-\Delta G_1$ were $0.54\,kJ \cdot mol^{-1}$ from C4 to C9, $1.02\,kJ \cdot mol^{-1}$ from C11 to C16, and the greatest change in the slope of $-\Delta G_1$ plots between C9 and C11, with $2.90\,kJ \cdot mol^{-1}$ (Fig. 5A). According to the report by Spector,[4] the deviation from linearity between C10 and C12 reflects the configrational adaptability of the albumin binding sites. However, all the other thermodynamic parameters also show a break in their trends at ten carbon units (C10). The absolute value of $-\Delta H$ of FFA increased linearly to a maximum at C9, but it was reduced with additional increasing alkyl chain length, and the value of $-\Delta H_{max}$ for complete binding of all sites on HSA increased largely from C9 to C11 as same as in the pattern of an increase in $-\Delta G_1$. Since the large negative value of ΔH_{max} represents the extent of the binding area for ligand binding to protein as described above, the chain length of FFA profoundly affects the binding location on a HSA molecule (Fig. 5). This large change at C10 may be explained by either: i) different primary binding sites for short- or medium-chain FFA ($\leqq$C9) and for long-chain FFA ($\geqq$C10), or ii) a common binding site for both groups but one which has a much greater affinity for FFA ($\geqq$C10).

The thermodynamic parameters can be interpreted in terms of the forces required to stabilize the FFA–HSA complex. From a purely pragmatic point of view, ΔG determines the direction of any spontaneous change in FFA–HSA equilibrium under specific conditions and can be brought about by either a decrease in ΔH, an increase in ΔS, or by a combination of both changes. The contribution to positive ΔH and ΔS arises from the occurence of a large degree of hydrophobic interaction, while the sources of negative ΔH and ΔS arise from van der Waals' interaction and hydrogen bonding formation. Although the electrostatic forces contribute to the positive ΔS, the value of ΔH is expected to be very small or almost zero for purely electrostatic interaction.[27]

The existence of an enthalpy–entropy compensation effect shows that a single mechanism predominates in the binding process,[37] and it is tempting to rationalize the linearities on the bases of the nature of the common binding sites. As shown in Fig. 6, the compensation plots for each class of binding sites on HSA molecule provide evidence that two different binding sites (two mechanisms) exist on the HSA molecule. Firstly, for the first class of binding sites for FFA ($\geqq$C10), the hydrophobic interaction plays an important role in stabilizing the FFA–HSA complexation, reflecting the small negative values of ΔS_{m1} and the constant ΔH_{m1} ($-48.0 \pm 0.48\,kJ \cdot mol^{-1}$). The longer-chain FFA has a greater freedom of rotation around its single bonds, and thus is more flexible. The increased freedom of movement allows the hydrocarbon side chain to be present on the surface of the HSA molecule (the more positive the ΔS), causing ΔG to be become more negative ($-1.02\,kJ \cdot mol^{-1}$ of CH_2 group). Secondly, for both the primary binding sites of FFA ($\leqq$C9) and the secondary binding sites of FFA ($\geqq$C10), the linear compensation plot with a slope approximately equal to the experimental temperature (310 K) was observed between ΔH_{mi} and ΔS_{mi}. Further, the van der Waals' interaction and hydrogen bonding formation in low dielectric media contribute to the binding with large negative values of ΔH_{mi} and ΔS_{mi}. Such interactions might be expected from the pK_a of FFA (4.3—4.9): it should exsist predominantly in an anionic form bound to HSA at pH 7.4, thus permitting the formation of hydrogen bonding with positively charged amino acid chains of HSA. The shorter chains have comparatively little freedom of movement, thus the influence of each additional methylene group to the van der Waals' interaction increases ΔH negatively with increasing chain length ($-7.47\,kJ \cdot mol^{-1}$ of CH_2 group) until the chain reached nine carbon units (C9). The formation of hydrogen bonding may restrict the rotational and transformational freedom of the alkyl-chain and fix it rigidly in the HSA molecule (the more negative the ΔS); thus the increments of $-\Delta G$ are small: $0.54\,kJ \cdot mol^{-1} \cdot CH_2^{-1}$ (the primary binding sites for C4 to C9) and $0.61\,kJ \cdot mol^{-1} \cdot CH_2^{-1}$ (the secondary binding sites for C11 to C16).

Our resuls support the proposal of separate high-affinity binding sites of long-chain and short- or medium-chain fatty acids,[3,15,16,21,23] and the findings in the present study are in agreement with the suggestion that the primary binding site for medium-chain FFA corresponds to a site in the second class for long-chain FFA.[22,23] FFA–HSA binding is dependent upon the balance of enthalpy and entropy changes (compensation), which may result in apparent linear relationships between thermodynamic functions and chain length. Thus, the clear disparity between FFA $\leqq$C9 and $\geqq$C11 in the thermodynamic parameters is interpreted as indicating the difference in the primary binding sites on the HSA molecule and/or the different interactions taking part in the complex formation of FFA with HSA.

References

1) T. Peters, Jr., *Adv. Protein Chem.*, **37**, 161 (1985).
2) D. J. Birkett and S. Wanwimolruk, "Protein Binding and Drug Transport," eds. by J. P. Tillement and E. Lindenlaub, F. K. Schattauer Verlag, Stuttgart, 1985, pp. 11—23.
3) U. Kragh-Hausen, *Pharmacol. Rev.*, **33**, 17 (1981).
4) A. A. Spector, *J. Lipid Res.*, **16**, 165 (1975).
5) D. S. Goodman, *J. Am. Chem. Soc.*, **80**, 3892 (1958).
6) J. D. Ashbrook, A. A. Spector and J. E. Fletcher, *J. Biol. Chem.*, **247**, 7038 (1972).
7) J. D. Ashbrook, A. A. Spector, E. C. Santos and J. E. Fletcher, *J. Biol. Chem.*, **250**, 2333 (1975).
8) J. F. Rodrigues de Miranda, T. D. Eikelboom and F. A. J. Van Os, *Mol. Pharmacol.*, **12**, 454 (1976).
9) N. A. Brown, A. G. E. Wilson and J. W. Bridges, *Biochem. Pharmacol.*, **31**, 4019 (1982).
10) T. Oida, *J. Biochem.* (Tokyo), **100**, 1533 (1986).

11) A. O. Perdersen, B. Hust, S. Andersen, F. Nielsen and R. Brodersen, *Eur. J. Biochem.*, **154**, 545 (1986).
12) A. O. Pedersen and R. Brodersen, *J. Biol. Chem.*, **263**, 10236 (1988).
13) B. Honoré and R. Andersen, *Anal. Biochem.*, **171**, 55 (1988).
14) C. B. Berde, B. S. Hundson, R. D. Simoni and L. A. Sklar, *J. Biol. Chem.*, **254**, 391 (1979).
15) S. M. Koh and G. E. Means, *Arch. Biochem. Biophs.*, **192**, 73 (1979).
16) I. Y. Lee and R. H. McMenamy, *J. Biol. Chem.*, **255**, 6121 (1980).
17) N. Hagag, R. A. McPherson, E. R. Birnbaum and D. W. Darnall, *J. Biol. Chem.*, **259**, 5411 (1984).
18) S. Gumpen, P. O. Hegg and H. Martens, *Biochim. Biophys. Acta*, **574**, 189 (1979).
19) A. A. Spector, E. C. Santos, J. D. Ashbrook and J. E. Fletcher, *Ann. N. Y. Acad. Sci.*, **226**, 247 (1973).
20) B. J. Soltys and J. C. Hsia, *J. Biol. Chem.*, **252**, 4043 (1977).
21) B. J. Soltys and J. C. Hsia, *J. Biol. Chem.*, **253**, 3023 (1978).
22) V. J. Cunningham, L. Hay and M. B. Stoner, *Biochem. J.*, **146**, 653 (1975).
23) U. Kragh-Hansen, *Biochem. J.*, **195**, 603 (1981).
24) K. Maruyama, S. Awazu, H. Nishigori and M. Iwatsuru, *Chem. Pharm. Bull.*, **34**, 3394 (1986).
25) K. J. Fehske, W. E. Müller and U. Woller, *Biochem. Pharmacol.*, **30**, 687 (1981).
26) A. A. Spector, *Methods Enzymol.*, **128**, 320 (1986).
27) P. D. Ross and S. Subramanian, *Biochemistry*, **20**, 3096 (1981).
28) L. H. M. Janssen and M. T. Van Wilgenburg, *Mol. Pharmacol.*, **14**, 884 (1978).
29) R. E. Johnson and R. L. Biltonen, *J. Am. Chem. Soc.*, **97**, 2349 (1975).
30) M. R. Eftink and R. L. Biltonen, "Biological Microcalorimetry," ed. by A. E. Beezer, Academic Press, New York, 1980, pp. 343—412.
31) H. J. Hinz, *Annu. Rev. Biophys. Bioeng.*, **12**, 285 (1983).
32) M. Otagiri, G. E. Hardee and J. H. Perrin, *Biochem. Pharmacol.*, **27**, 1401 (1978).
33) J. Fleitman and J. H. Perrin, *Int. J. Pharmaceut.*, **11**, 215 (1982).
34) J. H. M. Droge, L. H. M. Janssen and J. Wilting, *Biochim. Biophys. Acta*, **827**, 396 (1985).
35) R. Gill, C. Lopes, J. C. Sari and C. Briand, *Biochem. Pharmacol.*, **40**, 2241 (1990).
36) M. Yamamoto and H. Aki, *J. Biochem. Biophys. Methods*, **16**, 271 (1988).
37) H. Aki and M. Yamamoto, *J. Pharm. Pharmacol.*, **41**, 674 (1989).
38) H. Aki and M. Yamamoto, *Biochem. Pharmacol.*, **39**, 396 (1990).
39) H. Aki and M. Yamamoto, *J. Pharm. Pharmacol.*, **42**, 637 (1990).
40) H. Aki and M. Yamamoto, *Biochem. Pharmacol.*, **41**, 133 (1991).
41) M. Yamamoto, H. Aki and T. Wakabayashi, *Yakugaku Zasshi*, **101**, 443 (1981).